# Evaluation of *in vivo* cytogenetic toxicity of europium hydroxide nanorods (EHNs) in male and female Swiss albino mice

Vishnu Sravan Bollu, Susheel Kumar Nethi, Rama Krishna Dasari, Soma Shiva Nageshwara Rao, Sunil Misra & Chitta Ranjan Patra

# Nanotoxicology

ORIGINAL ARTICLE

# Evaluation of *in vivo* cytogenetic toxicity of europium hydroxide nanorods (EHNs) in male and female Swiss albino mice

Vishnu Sravan Bollu[1#], Susheel Kumar Nethi[1,2#], Rama Krishna Dasari[2,3], Soma Shiva Nageshwara Rao[2,3], Sunil Misra[2,3], and Chitta Ranjan Patra[1,2]

[1]Biomaterials Group, CSIR – Indian Institute of Chemical Technology, Tarnaka, Hyderabad, Telangana State, India, [2]Academy of Scientific and Innovative Research (AcSIR), Chennai, India, and [3]Toxicology Unit, Biology Division, CSIR – Indian Institute of Chemical Technology, Tarnaka, Hyderabad, Telangana State, India

## Abstract

Our group already demonstrated that europium hydroxide nanorods (EHNs) show none or mild toxicity in C57BL/6 mice even at high dose and exhibited excellent pro-angiogenic activity towards *in vitro* and *in vivo* models. In the present study, we evaluated the *in vivo* cytogenetic toxicity of intraperitoneally administered EHNs (12.5–250 mg/kg/b.w.) in male and female Swiss albino mice by analyzing chromosomal aberrations (CAs), mitotic index (MI), micronucleus (MN) from bone marrow and peripheral blood. Furthermore, we performed the cytogenetic toxicity study of EHNs towards Chinese hamster ovary (CHO) cells, in order to compare with the *in vivo* results. The results of CA assay of mice treated with EHNs (12.5–125 mg/kg/b.w.) showed no significant change in the formation of aberrant metaphases compared to the control group. Also, there was no significant difference in the number of dividing cells between the control group and EHNs-treated groups observed by MI study, suggesting the non-cytotoxicity of EHNs. Additionally, FACS study revealed that EHNs do not arrest cells at any phase of cell cycle in the mouse model. Furthermore, MN test of both bone marrow and peripheral blood showed no significant differences in the induction of MNs when compared with the control group. *In vitro* results from CHO cells also support our *in vivo* observations. Considering the role of angiogenesis by EHNs and the absence of its genotoxicity in mouse model, we strongly believe the future application of EHNs in treating various diseases, where angiogenesis plays an important role such as cardiovascular diseases, ischemic diseases and wound healing.

## Introduction

Nanotechnology has been widely used in every field of science and technology, including biology and medicine, due to their fundamental unusual physicochemical properties in the nanoscale range (Boisselier & Astruc, 2009). Since the last decade, extensive research is being carried out for the development of therapeutic and diagnostic nanomedicine that could be beneficial for curing several diseases such as cancer, cardiovascular related diseases (CVD), arthritis, alzheimer's disease and various others (Alivisatos, 2004; Boisselier & Astruc, 2009; Gao et al., 2004; Mulder & Fayad, 2008; Nethi et al., 2014; Patra et al., 2008b, 2011; Sung et al., 2011; Wei et al., 2014; Yan et al., 2012). Nanomaterials including several metal nanoparticles such as gold, silver, platinum, zinc oxide, zircona, iron oxide, calcium phosphate, titanium oxide, europium hydroxide, biodegradable polymers have been extensively studied for their biomedical applications (Barui et al., 2012; Boisselier & Astruc, 2009; Dai et al., 2012; Giljohann et al., 2010; Kumar et al., 2008; Liu & Zhang, 2012; Obregon et al., 2013; Patra et al., 2008b, 2011; Piao et al., 2011; Porcel et al., 2010; Wei et al., 2014). However, the non-toxic behavior of these nanomaterials cannot be extrapolated to the clinical applications based on their *in vitro* cell-based studies. Therefore, the use of nanomaterials may have long-term unknown hazards to human health and environment. In this context, a precise toxicological assessment of these potential nanomaterials and therapeutic drugs is very important to safeguard the human life and the environment (Coccini et al., 2013).

Recently, we have demonstrated the pro-angiogenic properties of EHNs [$Eu^{III}(OH)_3$] and assessed the non-toxic nature towards *in vitro* and *in vivo* models (Nethi et al., 2015; Patra et al., 2008a, 2009, 2011; Wei et al., 2014). Considering the huge impact of angiogenesis on our healthcare system, the pro-angiogenic EHNs could be developed as an alternative treatment strategy for CVDs, ischemic diseases and wound healing, where angiogenesis plays a key role. In order to establish an efficient and effective treatment strategy for CVDs using EHNs, its feasibility, bio-safety and bioavailability should be investigated in detail. In this context, we have already reported the detailed short-term and long-term

#Both the authors contributed equally.

Correspondence: Dr. Sunil Misra, Toxicology Unit, Biology Division, CSIR – Indian Institute of Chemical Technology (CSIR-IICT), Uppal Road, Tarnaka, Hyderabad 500 007, Telangana State, India. Tel: +91 4027191379. E-mail: smisra@iict.res.in

Dr. Chitta Ranjan Patra, Biomaterials Group, CSIR – Indian Institute of Chemical Technology (CSIR-IICT), Uppal Road, Tarnaka, Hyderabad 500 007, Telangana State, India. Tel: +91 4027191480. Fax: +91 4027160387. E-mail: crpatra@iict.res.in or patra.chitta@gmail.com

*in vivo* toxicity of EHNs in C57BL/6 mice by analyzing the blood hematology, serum clinical chemistry and histological examination of vital organs (liver, kidney, spleen and lungs) and found none or mild toxicity of EHNS even at high doses (125 mg/kg b.w./day) (Patra et al., 2009). However, several reports demonstrate that nanoparticles with different size, shape and surface coatings have been proven to be genotoxic and cytotoxic to mammalian cells (Dhawan et al., 2006; Lewinski et al., 2008; Tsuji et al., 2006). Since nanoparticles have been widely used for biomedical applications and healthcare especially drug delivery, medical imaging pharmaceuticals, therefore nanotoxicology research that refers to the study of toxic effects of nanomaterials on genomic stability and integrity, is now gaining attention (Tsuji et al., 2006). In order to develop an efficient alternative treatment strategy for CVDs using EHNs, its bio-safety should be well established using various toxicological evaluations. Therefore, in the present work, we investigated the in-detailed *in vivo* cytogenetic toxicity of EHNs in male and female Swiss albino mice and compared the results with *in vitro* genotoxic evaluation of EHNs in CHO cells using several standard genotoxicity assays.

## Materials and methods

### Materials

Europium nitrate hydrate [Eu(NO$_3$)$_2 \cdot$H$_2$O] and aqueous ammonium hydroxide [aq.NH$_4$OH, 28–30%] were purchased from Sigma-Aldrich (St. Louis, MO) and used for the synthesis of Eu$^{III}$(OH)$_3$ nanorods (EHNs) without any further purifications. Laboratory grade reagents like methanol, ethanol, acetic acid, sodium citrate and tris-EDTA were obtained from SD Fine Chemicals, Mumbai, India and HiMedia, Mumbai, India. MTT (3-(4,5-dimethylthiazol-2-yl)-2,5-diphenyltetrazolium bromide) has been purchased from Sigma-Aldrich, St. Louis, MO. Mitomycin-C (MMC) has been procured from BioPharma Pvt. Ltd., Hyderabad, India. Giemsa stain and colchicine were procured from Loba Chemicals, Mumbai, India and cyclophosphamide (CP) from Zydus, Ahmedabad, India.

### Microwave synthesis of Eu$^{III}$(OH)$_3$ nanorods (EHNs)

EHNs were synthesized using a microwave irradiation method according to our reported work (Patra et al., 2011). The synthesis was performed in a modified domestic microwave oven (MWO) (Samsung MW73BD, Suwon, South Korea) fitted with a condenser and circulating water-cooling system. Aqueous europium(III) nitrate solution was allowed to react with aq.NH$_4$OH at under a closed system. In the synthesis procedure, 39 mL of 0.05 M aqueous europium(III) nitrate solution at [OH/Eu] = 4 molar ratio was taken and reacted with 1 mL of aqueous NH$_4$OH resulting in a white colloidal mixture. The resultant mixture was irradiated at 600 W for 60 min in MWO to obtain the final EHNs. After synthesis, the resulting nanoparticles suspension was centrifuged at 6000 rpm and washed with Millipore water and suspended in ethanol overnight to remove traces of unreacted aq.NH$_4$OH. It was followed by centrifugation and washing with water to remove ethanol completely and the nanoparticles suspension was dried in a hot air oven to obtain the final compound.

### Characterization techniques

#### X-ray diffraction (XRD)

XRD analysis was performed to identify the structure and phase purity of the as-synthesized EHNs using a Bruker AXS D8 Advance Powder X-ray diffractometer (Billerica, MA) (using Cu Kα $\lambda$ = 1.5406 Å radiation).

#### Fourier transformed infrared spectroscopy (FTIR)

The functional group analysis of the as-synthesized nanorods was performed using FTIR to confirm their identity. The FTIR spectrum of the sample was recorded using thermo Nicolet Nexus 670 spectrometer (Minneapolis, MN) in the diffuse reflectance mode at a resolution of 4 cm$^{-1}$ in KBr pellets.

#### Transmission electron microscopy (TEM)

The morphology and size of nanorods were examined on a JEOL (Tokyo, Japan) instrument operated at 200 kV. The particle size distribution of as-synthesized EHNs in 1× Tris-EDTA suspension and EHNs incubated in mouse serum for different time points (6–48 h) was calculated from the TEM images using IMAGE J software (NIH, Bethesda, MD).

#### Dynamic light scattering (DLS)

The average particle size of EHNs incubated in mouse serum in a time-dependent manner (6–48 h) was analyzed by DLS phenomena and recorded using FAST Version 2.7.1 (Alango Ltd., Tirat Carmel, Israel).

#### Surface area analysis

The surface area of the EHNs was estimated using N$_2$ adsorption isotherms at $-196\,^\circ$C by the multipoint Brunauer–Emmett–Teller (BET) method, considering 0.162 nm$^2$ as its cross-sectional area using Autosorb 1C (Quantachrome Instruments, Boynton Beach, FL) (Sreedhar et al., 2015).

### Preparation of EHNs suspension

The required amount of nanorods powder was taken in a sterile motor and pestle and grounded finely by adding 1× TE buffer and mixed thoroughly to make a fine suspension. The nanorods suspension was subjected to sonication and administered to mice through intraperitoneal route accordingly in a dose-dependent manner (12.5–250 mg/kg/b.w.).

### *In vitro* experiments

The Chinese hamster ovary (CHO) cells were obtained from ATCC (Manassas, VA). The cells were grown in DMEM medium supplemented with 10% fetal bovine serum and 0.005% antibiotics such as penicillin, streptomycin and kanamycin. The cells were grown in a humidified incubator at 37 $^\circ$C and 5% CO$_2$. In all the experiments, MMC was used as a positive control experiment (Mazumdar et al., 2011). The MTT assay towards CHO cells was performed according to our standard protocol (Nethi et al., 2015). All *in vitro* cytogenetic experiments have been described in the Supporting Information (Di Virgilio et al., 2010; Franchitto et al., 1998; Hittelman & Rao, 1974).

### *In vivo* cytogenetic toxicity study

#### Animals

Swiss albino mice aged 4–5 weeks (weight ∼20–25 g) were procured from National Institute of Nutrition (NIN), Hyderabad, India. Mice were acclimatized for one week prior to experimentation. All animal studies were performed based on the approval by Institutional Animal Ethics Committee (IAEC Approval No. IICT/BIO/TOX/SM/20/12/2013/09), CSIR-IICT, India.

#### Experimental design

Initially, Swiss albino mice were categorized in to male and female groups. Male and female mice were randomly arranged

(three males and three females in each cage) into five different experimental groups, viz. Gr-I: Control: 0.9% NaCl, Gr-II: EHNs: 12.5 mg/kg/b.w., Gr-III: EHNs: 125 mg/kg/b.w., Gr-IV: EHNs: 250 mg/kg/b.w. and Gr-V: positive control group with CP: 40 mg/kg/b.w. and injected i.p. The dose of CP has been selected based on the previous reported literature (Li et al., 2011). The doses of EHNs were selected based on previous *in vivo* toxicity study in C57BL/6 mice (Patra et al., 2009). The genotoxicity data for male and female mice were recorded separately to understand the sex-specific susceptibility of test compounds. Additionally, we have also performed the cell cycle analysis of bone marrow cells isolated from Swiss albino male mice using FACS analysis.

*End points selected for toxicity studies.* Mitotic metaphase chromosomal aberrations (CAs) and mitotic index (MI) studies were done after 24 h post-treatment from bone marrow cells. Two separate sources were selected and examined for micronuclei (MNs test), i.e. 30 h post-treatment from both peripheral blood and bone marrow cells.

### Cell cycle analysis

The *in vivo* bone marrow cell cycle analysis was performed as previously reported (Rithidech et al., 2008). Briefly, the 3–4 weeks old male Swiss albino mice have been injected i.p. with treatments (0.9% NaCl, EHNs: 12.5 mg/kg; 125 mg/kg; 250 mg/kg & CP: 40 mg/kg b.w.). Colchicinized mice were sacrificed and bone marrow from tibia and femur was flushed out using ice cold 1X PBS. The cells were washed twice to remove the excess fat and adherent tissues by centrifugation at 2000 rpm for 5 min and fixed overnight in 70 % ethanol at $-20\,^{\circ}$C. Next day the cells were washed by centrifugation with 1X PBS and then stained using propidium iodide (PI) solution supplemented with RNAse and triton-X, for 45 min at room temperature. After staining, the cells were washed with 1X PBS to remove the unbound PI and then cell cycle analysis was performed using BD FACS Canto, USA.

### In vivo *CA assay*

The CAs assay was performed to analyze the genotoxic potential of any chemical compound or a material (Ishidate et al., 1998). The bone marrow CA assay was performed as described in previous reports (Adler, 1980; Misra & Choudhury, 2006). In brief, the femur and tibia bones were dissected and bone marrow was flushed into hypotonic solution (0.9% sodium citrate). The resulting cell suspension was mixed thoroughly with Pasteur pipette, incubated at $37\,^{\circ}$C for 25–30 min, and finally centrifuged at 2000 rpm for 5 min. The cell pellets were re-suspended in methanol/acetic acid (3:1 v/v) after discarding the supernatant. This procedure was repeated twice. The cell suspension was dropped on clean, non-greasy, pre-chilled slides using the flame-drying technique and stained with Giemsa in Sorensen' buffer (pH = 6.8). At least 300 well spread mitotic chromosomal plates per treatment were scanned microscopically for the presence of CAs such as chromatids gaps & breaks, chromosome gaps & breaks, exchanges, fragments, pulverization, rings and minutes.

### Mitotic index

Mitotic index (MI) is a parameter that helps to measure the cell division status (Killmann et al., 1963). It is useful for characterizing cell proliferation status where it indicates the growth and multiplication, leading to establishment of tissues. Mitotic index is directly proportional to the proliferation of cells during cell division (Clahsen et al., 1999). It is measured by taking the ratio of number of dividing cells to the total number of

cells observed. The slides prepared for CA assay were used for evaluating MI. At least 2000 cells were randomly scanned for the presence of dividing cells per each animal.

### In vivo *MN assay*

The MN assay is a primary standard test for evaluation of genotoxicity for accessing the safety of any material (Krishna & Hayashi, 2000). It has been well established that the frequency of MNs formation caused by any substance, is directly related to its carcinogenic potential, it can also be considered as a biomarker for cancer (Bonassi et al., 2007). MNs in polychromatic erythrocytes (PCEs) were scanned manually from both bone marrow and peripheral blood of mice (30 h post-treatment) according to the modified procedure (Schmid, 1975).

*MN assay using bone marrow PCE.* After 30 h post-treatment, bone marrow MN test was performed according to our published literature (Balasubramanyam et al., 2009; Choudhury et al., 2000). Briefly, the bone marrow sample was collected by flushing the femur and tibia bones with 1% sodium citrate at 6–8 °C and mixed thoroughly with Pasteur pipette. After incubation, the cells were centrifuged at 1200 rpm for 5 min. Finally, the supernatant was discarded and smeared on clean grease free slides. Four slides were prepared from each mouse, air dried and incubated at 37 °C for 24 h. Next day, the slides were dipped in methanol for 2–3 min, air dried and stained with Giemsa in Sorensen' buffer (pH 6.8) for 10 min. Around 2000 PCEs per mouse from all randomly selected slides were scored for the frequency of MN in the bone marrow PCEs.

*MN assay using peripheral blood PCE.* The blood was collected from each mouse through tail vein puncture following proper anesthetic procedure and four slides (blood smear) were prepared for each animal. All the slides were allowed to dry and incubated in humidified chamber for 24 h at 37 °C followed by dipping in methanol for 2–3 min, air dried and stained with 0.5% Giemsa in Sorensen' buffer (pH 6.8) for 10 min. The slides were then washed and observed in light microscope (1000× magnification). At least 2000 PCE were scored randomly per animal from all the four-coded slides and MNs were recorded.

## Bio-distribution of EHNs in Swiss albino mice

The toxicokinetics study was conducted at two different time intervals, i.e. 6 and 24 h post-treatment of EHNs. We have carried out ICP-OES analysis for the detection of europium in blood (circulation system/target cells) and bone marrow (target cells/tissue) of Swiss albino male ($n = 3$) and female ($n = 3$) mice administered with the highest dose of EHNs (250 mg/kg b.w.). ICP-OES analysis was conducted to detect the bioavailability of EHNs in vital organs including liver, kidney and spleen along with blood, bone marrow and feces according to the published literature (Tiwari et al., 2014). In order to get the maximum bio-availability of EHNs in different tissues as well as in feces, we have pooled the both male and female tissues, blood, bone marrow (after 6 and 24 h post-treatment) and feces (collected after 24 h post-treatment) for ICP-OES analysis. All vital organs, bone marrow, blood and feces were weighed and digested in 75% $HNO_3$ for 48–72 h. Furthermore, the obtained solution was filtered using a 0.22-μm syringe filter and diluted with Millipore water and submitted for ICP-OES analysis.

## Statistical analysis

All the data were analyzed with unpaired Student's *t*-test, followed by ''One-way ANOVA'' with Dunnett's post-test performed using Graph Pad Prism version 6.04 for Windows, Graph Pad Software, San Diego, CA.

## Results

### Synthesis and characterization of EHNs

The EHNs were synthesized using an advanced microwave synthesis technique as previously reported by our group (Patra et al., 2011) and the nanomaterial was thoroughly characterized by several analytical tools. The structure and phase purity of the as-synthesized EHNs was investigated using the XRD analysis. The XRD analysis (Figure S1) showed the crystalline nature of EHNs, where all the diffraction peaks indexed to a hexagonal phase of nanorods (Patra et al., 2011). The FTIR analysis was performed in order to determine and characterize the functional groups. The FTIR spectrum of EHNs (Figure S2) demonstrated the presence of characteristic peaks at 3421 and 671 cm$^{-1}$, which are attributed to the O–H bond stretching frequency, which confirmed the presence of –OH functional group in EHNs. TEM analysis was carried out to determine the shape and morphology of EHNs. The surface area of EHNs was measured employing BET theory using the N$_2$ physisorption method and was found to be around 5 m$^2$/g.

The TEM image of EHNs in Figure S3(a) clearly indicated the rod shape of the europium hydroxide nanoparticle. We calculated the particle size distribution from TEM images considering many particles of EHNs suspended in 1× TE buffer using IMAGE J software and presented in Figure S3(b)–(c). The histograms (Figure S3b–c) show that particles size distribution of EHNs is in the range of 200–300 nm in length and 40–80 nm in diameter. All results together confirm that as-synthesized materials are crystalline europium hydroxide nanorods (EHNs: Eu$^{III}$(OH)$_3$].

### Summary of all *in vitro* and *in vivo* experiments

The overall summary of physico-chemical characterization of EHNs and their *in vitro* cytotoxicity (MTT assay) and genotoxicity study, evaluation of *in vivo* genotoxicity (CA assay, MI, MN test), cell cycle analysis by FACS and the bio-distribution of EHNs in vital organs (liver, kidney, spleen), blood and bone marrow of Swiss albino mice along with feces is presented in Table 1.

### Cell cycle analysis

The cell cycle analysis was done in order to evaluate the dose-dependent effect of EHNs on different phases of cell cycle. The Swiss male mice were treated with EHNs at different doses of 12.5 mg/kg, 125 mg/g and 250 mg/kg for 24 h and the bone marrow cells were processed for cell cycle analysis. The results represented in Figure 1(a)–(f) clearly revealed that the EHNs do not induce cell cycle arrest at different doses, in mouse bone marrow cells at any phase of cell cycle, which was evident from the similar cell population in G0/G1, S and G2/M phases. However, the positive control CP induced S-phase cell cycle arrest observed by accumulated cell population in G2/M phase (Schwartz & Waxman, 2001). The percentage of cell population in different phases of G0/G1, S and G2/M phases of cell cycle (Figure 1f) in bone marrow cells isolated from mice treated with various doses of EHNs (12.5–250 mg/kg/b.w.) does not show any difference in the cell population of these phases. The results altogether suggest that the EHNs do not induce any cell cycle arrest and show inconsiderable cytotoxicity even at higher doses, suggesting their high biocompatibility towards *in vivo* model.

### *In vivo* CA assay

Bone marrow mitotic metaphase chromosome aberrations (CAs) assay was carried out after 24 h post-treatment in male ($n = 3$) and female ($n = 3$) Swiss mice. The results are presented in Table 2

and Figure S4, where Figure S4(a)–(c) represents female group data and Figure S4(d)–(f) represents male group data. The CAs were mostly of chromatid gaps and breaks type, chromosome breaks, fragments and minutes. In the negative control group (Gr I: treatment with 0.9% NaCl), a very low incidence of CAs was observed, where 12 aberrant metaphases of 465 in female and 13 aberrant metaphases of 412 in males were scanned (Table 2). In this group, the CAs were mostly of chromatid and chromosome type gaps. The positive control mice treated with CP (Gr. V: 40 mg/kg b.w.) showed 239 aberrant metaphases of 377 scanned in female (63.5%) and 219 aberrant metaphases of 427 (51.2%) in males.

A low incidence of aberrant metaphase spreads was observed in 12.5 mg/kg EHNs treated groups (Gr. II), where 28 spreads in female of 336 and 16 spreads in male of 425 were found to be aberrant. The major types of CAs were of chromatid type gaps and breaks both in females (gaps: 22 and breaks: 20) and males (gaps: 9 and breaks: 9). Similarly, the mice treated with 125 mg/kg of EHNs (Gr. III) showed 57 aberrant metaphases of 651 in female and 18 of 256 in males. The majority of the CAs were of chromatid type gaps in both females (gaps: 28 and breaks: 37) and males (gaps: 15 and breaks: 7). However, all the results up to 125 mg/kg b.w. treatment were not statistically significant. In the highest dose of EHNs treated mice, i.e. 250 mg/kg b.w. (Gr. IV), a high incidence of 59 aberrant metaphases of 436 metaphase spreads were observed in females and 112 of 620 in males. Chromatid type gaps and breaks were the major CAs observed in females (gaps: 19 and breaks: 47) and males (gaps: 67 and breaks: 103). In this treatment group, the minutes were also one of the major aberrations observed in female mice group. The total aberrations excluding gaps in this group showed a statistically significant difference in comparison with the negative control group in both females ($p < 0.001$) and males ($p < 0.005$) while treated with 250 mg/kg b.w. dose of EHNs. The Gr. II (12.5 mg/kg) and Gr. III (125 mg/kg) did not show any difference in the total aberrations (both including and excluding gaps) in comparison with the negative control group, whereas the Gr. IV (250 mg/kg) showed a significant difference in comparison with the negative control, which signified that the EHNs started showing its genotoxic effects at the highest dose (250 mg/kg) which is even ∼5 times lower than that of the positive control group (Gr. V: 40 mg/kg of CP) in female mice and ∼3 times lower in male mice (Table 2). However, at lower dose/therapeutic dose (12.5 mg/kg b.w.) the aberrations were not significant and ∼15 times lower than that of the positive control. Again, the positive control group showed a highly statistical significant difference when compared with the negative control group ($p < 0.0001$). The graphical representation of the percentage of aberrant metaphases observed in all the three doses from both male and female Swiss albino mice are represented in Figure S4(a)–(f). Figure S5 shows the representative images of normal and aberrant chromosomal metaphase spreads.

### Mitotic index in bone marrow cells

Bone marrow MI study after 24 h post-treatment showed no significant difference in the negative and positive control treatments of both male and female mice groups as shown in Table 3 and Figure S6. However, the group treated with 12.5 mg/kg b.w. of EHNs showed less percentage of MI compared to the negative control but the difference was not statistically significant. Interestingly, two higher doses of EHNs did induce slightly increase in frequency of dividing cells compared to that of the negative control but was not found to be statistically significant. The graphical representation of the tabular results of MI of both male and female Swiss albino mice is shown in Figure S6.

Table 1. Tabular summary of the physico-chemical characterization and *in vitro*, *in vivo* genotoxic assessment, cell cycle analysis and bio-distribution study of EHNs in CHO cells and Swiss albino mice.

**Physicochemical characterization of EHNs**

| Technique | Result |
| --- | --- |
| TEM | Nanorods, length: 200–300 nm and width: 40–80 nm |
| XRD | Crystalline - hexagonal phase |
| FTIR | OH stretching frequency |
| BET | Surface area around 5 m²/g |

**MTT assay:** The EHNs at concentrations 1–50 µg/mL showed good cell viability and biocompatibility *in vitro*.

**In vitro genotoxicity assays (CHO cells)**

Chromosomal aberration assay

| | Control | 5 µg/ml | 10 µg/ml | 20 µg/ml | MMC |
| --- | --- | --- | --- | --- | --- |
| % Aberrant M | 8.6 | 10.9$^{ns}$ | 16.8$^{ns}$ | 23.1** | 25.9** |
| TA–gaps/100 M | 5.0 | 4.3$^{ns}$ | 7.6$^{ns}$ | 13.7$^{ns}$ | 33.8*** |

Micronucleus assay

| Control | 5 µg/ml | 10 µg/ml | 20 µg/ml | MMC |
| --- | --- | --- | --- | --- |
| 3.6 | 4.9$^{ns}$ | 4.5$^{ns}$ | 6.6$^{ns}$ | 16.8*** |

Mitotic Index

| Control | 5 g/ml | 10 µg/ml | 20 µg/ml | MMC |
| --- | --- | --- | --- | --- |
| 9.1 | 8.4$^{ns}$ | 4.9$^{ns}$ | 4.7$^{ns}$ | 3.7$^{ns}$ |

**In vivo genotoxicity assays (MSA)**

Chromosomal aberration assay

| | 0.9% NaCl | 12.5 µmg/kg | 125 mg/kg | 250 mg/kg | CP |
| --- | --- | --- | --- | --- | --- |
| % Aberrant M | 3.2 | 3.9$^{ns}$ | 6.1$^{ns}$ | 17.9** | 51.0** |
| TA–gaps/100 M | 0.4 | 2.1$^{ns}$ | 3.5$^{ns}$ | 19.1* | 84.3*** |

Micronucleus assay

| | 0.9% NaCl | | 12.5 mg/kg | | 125 mg/kg | | 250 mg/kg | | CP | |
| --- | --- | --- | --- | --- | --- | --- | --- | --- | --- | --- |
| | PB | BM | PB | BM | PB | BM | PB | BM | PB | BM |
| | 1.4 | 3.4 | 0.5$^{ns}$ | 2.2$^{ns}$ | 0.2$^{ns}$ | 2.3$^{ns}$ | 0.5$^{ns}$ | 1.6** | 16.9** | 25.5** |

Mitotic Index

| 0.9% NaCl | 12.5 mg/kg | 125 mg/kg | 250 mg/kg | CP |
| --- | --- | --- | --- | --- |
| 2.9 | 2.5$^{ns}$ | 3.0$^{ns}$ | 5.0$^{ns}$ | 3.3$^{ns}$ |

**In vivo genotoxicity assays FSA**

Chromosomal aberration assay

| | 0.9% NaCl | 12.5 mg/kg | 125 mg/kg | 250 mg/kg | CP |
| --- | --- | --- | --- | --- | --- |
| % Aberrant M | 2.5 | 5.2$^{ns}$ | 11.2$^{ns}$ | 13.9** | 63.5*** |
| TA–gaps/100 M | 0.8 | 4.6$^{ns}$ | 9.2$^{ns}$ | 19.3** | 115.0*** |

Micronucleus assay

| | 0.9% NaCl | | 12.5 mg/kg | | 125 mg/kg | | 250 mg/kg | | CP | |
| --- | --- | --- | --- | --- | --- | --- | --- | --- | --- | --- |
| | PB | BM | PB | BM | PB | BM | PB | BM | PB | BM |
| | 0.9 | 1.9$^{ns}$ | 0.2$^{ns}$ | 1.5$^{ns}$ | 0.2$^{ns}$ | 1.7$^{ns}$ | 0.8$^{ns}$ | 1.6** | 10.1* | 15.6*** |

**Biodistribution Eu (g/g) MSA and FSA ICP-OES**

| Organ | 6h | 24h |
| --- | --- | --- |
| Liver | 8.75 | 23.74 |
| Spleen | 45.22 | 106.89 |
| Kidney | 3.03 | 3.13 |
| Blood | 1.19 | BD |
| Bone marrow | 1.09 | BD |
| Feces | BD | 12.00 |

**CCA of MSA using FACS:** The cell cycle analysis demonstrated that bone marrow cells isolated from male Swiss mice do not show arrest of cells at any phase ($G_0/G_1$, $S$ and $G_2/M$) of cell cycle.

TEM, transmission electron microscopy; XRD, X-ray diffraction; FTIR, Fourier transformed infrared radiation; BET, Brunauer–Emmett–Teller; MMC, mitomycin-C; M, metaphase; TA, Total aberrations, TA-gaps, total aberrations excluding gaps; MSA, male Swiss albino mice; CP, [cyclophosphamide]; ICPOES, inductively coupled plasma optical emission spectrometry; BD, below detection limit, CCA, cell cycle analysis; FACS, Fluorescence-activated cell sorting, ns: non-significant.

*Significantly different from control at $p < 0.05$.
**Significantly different from control at $p < 0.001$.
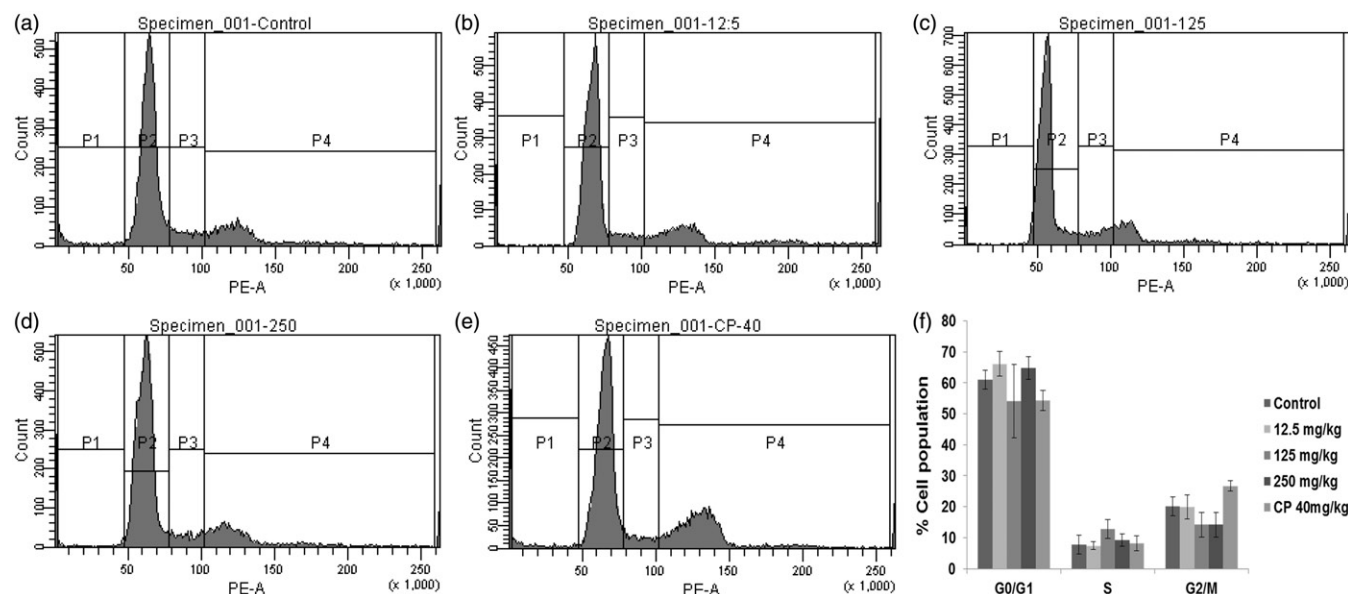***Significantly different from control at $p < 0.0001$.

Figure 1. Cell cycle analysis of bone marrow cells isolated from male Swiss albino mice treated with different doses of EHNs. (a) Control: 0.9% NaCl, (b) 12.5 mg/kg b.w., (c) 125 mg/kg b.w. and (d) 250 mg/kg b.w., performed using flow cytometry. (e) CP: cyclophosphamide (40 mg/kg b.w.) is used as a positive control experiment. (f) Histogram represents the percentage of cell population in G0/G1, S and G2/M phases of cell cycle. The population of cells in different phases represented as P1 – apoptotic region (sub G0/G1), P2 – G0/G1 phase, P3 – S phase and P4 – G2/M phase of cell cycle.

Table 2. Frequency of CAs in bone marrow cells of Swiss mice at 24 h post-EHNs treatment.

| Treatment | Dose mg/kg b.w. | No. of mice treated /sex | No. of metaphase examined | No. of aberrant metaphases | Chromatid type G | Chromatid type B | Chromosome type G | Chromosome type B | F/M | TA/TA-gap | % of aberrant metaphase | TA + gaps/100 metaphases (M $\pm$ SEM) | TA-gaps/100 metaphases (M $\pm$ SEM) |
|---|---|---|---|---|---|---|---|---|---|---|---|---|---|
| 0.9% | – | 3 ♀ | 465 | 12 | 10 | – | 2 | – | 3/– | 17/3 | $2.5 \pm 0.6$ | $3.4 \pm 0.7$ | $0.8 \pm 0.6$ |
| NaCl | | 3 ♂ | 412 | 13 | 12 | 2 | – | – | – | 14/2 | $3.2 \pm 0.4$ | $3.4 \pm 0.4$ | $0.4 \pm 0.4$ |
| EHNs | 12.5 | 3 ♀ | 336 | 28 | 22 | 20 | 1 | – | 4/1 | 50/25 | $5.2 \pm 3.1^{ns}$ | $9.3 \pm 5.2^{ns}$ | $4.6 \pm 2.8^{ns}$ |
| | | 3 ♂ | 425 | 16 | 9 | 9 | – | – | – | 18/9 | $3.9 \pm 1.5^{ns}$ | $4.4 \pm 1.7^{ns}$ | $2.1 \pm 0.4^{ns}$ |
| | 125 | 3 ♀ | 651 | 57 | 28 | 37 | – | 1 | 6/3 | 79/51 | $11.2 \pm 4.3^{ns}$ | $14.7 \pm 5.8^{ns}$ | $9.2 \pm 3.6^{ns}$ |
| | | 3 ♂ | 256 | 18 | 15 | 7 | – | – | 2/– | 24/9 | $6.1 \pm 2.7^{ns}$ | $9.7 \pm 3.4^{ns}$ | $3.5 \pm 1.2^{ns}$ |
| | 250 | 3 ♀ | 436 | 59 | 19 | 47 | 5 | 2 | 1/17 | 115/86 | $13.9 \pm 2.1^{**}$ | $24.9 \pm 4.5^{**}$ | $19.3 \pm 3.0^{**}$ |
| | | 3 ♂ | 620 | 112 | 67 | 103 | 2 | 5 | 5/3 | 195/124 | $17.9 \pm 2.9^{**}$ | $29.9 \pm 6.1^{*}$ | $19.1 \pm 4.8^{*}$ |
| CP | 40 | 3 ♀ | 377 | 239 | 56 | 75 | 15 | 20 | 205/48 | 502/416 | $63.5 \pm 6.1^{***}$ | $134.6 \pm 14.2^{***}$ | $115.0 \pm 11.2^{***}$ |
| | | 3 ♂ | 427 | 219 | 87 | 104 | 22 | 06 | 158/37 | 479/348 | $51.2 \pm 2.2^{***}$ | $109.2 \pm 9.5^{***}$ | $84.3 \pm 9.4^{***}$ |

b.w., Body weight; G, gaps; B, breaks; F, fragments; M, minutes; E, exchange, TA, total aberrations, TA-gap, total aberrations excluding gaps; M $\pm$ SEM, Mean $\pm$ standard error of mean. Control, 0.9% NaCl; CP, cyclophosphamide (positive control); ns, non-significant.
*Significantly different from control at $p < 0.05$.
**Significantly different from control at $p < 0.001$.
***Significantly different from control at $p < 0.0001$.

### *In vivo* MN assay

#### *Bone marrow MN test*

Both male and female mice groups of the positive control exhibited significantly higher number of MNs per 1000 PCEs in female 15.6 ($p < 0.0001$) and in male 25.5 ($p < 0.001$) compared to the negative control group of female ($1.9 \pm 0.5$) and male ($3.4 \pm 0.7$) per 1000 PCEs. Figure 2 and Table S1 represent the results of bone marrow MN assay in both female (Figure 2a) and male (Figure 2b) Swiss albino mice. The group that received 12.5 mg/kg EHNs treatment did not show any significant difference in MN-PCE per 1000 PCE in female ($1.4 \pm 0.7^{ns}$) and male ($2.2 \pm 0.6^{ns}$) in comparison with the negative control. The mice

group treated with 125 mg/kg EHNs also exhibited a similar result of insignificant difference in female ($1.5 \pm 1.0^{ns}$) and male ($2.3 \pm 1.1^{ns}$) when compared with that of mice group treated with the negative control. Moreover, no significant difference was observed in the highest dose treatment group (250 mg/kg) in female ($1.7 \pm 0.1^{ns}$) and male ($1.6 \pm 1.1^{ns}$) in comparison with the negative control group. So, altogether, the three groups that received three different doses of EHNs were found to induce less number of MNs in both female (Figure 2a) and male (Figure 2b) compared to the negative group and the difference was found to be non-significant. By these results we could infer that EHNs treatment do not induce major genotoxicity at the MN level. The graphical representation of the tabular results of bone marrow

Table 3. Percentage of mitotic index (MI) in bone marrow cells of Swiss mice at 24 h post-treatment.

| Name of chemical | Dose mg/kg b.w. | No. of mice/sex | No. of cells examined | No. of dividing cells | % of dividing cells (MI) (M ± SEM) |
|---|---|---|---|---|---|
| NaCl | 0.9% (v/v) | 3 ♀ | 3427 | 76 | $2.1 \pm 0.1$ |
|  |  | 3 ♂ | 3603 | 108 | $2.9 \pm 0.1$ |
| EHNs | 12.5 | 3 ♀ | 5947 | 101 | $1.8 \pm 0.4^{\text{ns}}$ |
|  |  | 3 ♂ | 5391 | 135 | $2.5 \pm 0.3^{\text{ns}}$ |
|  | 125 | 3 ♀ | 5991 | 158 | $3.2 \pm 0.7^{\text{ns}}$ |
|  |  | 3 ♂ | 5850 | 174 | $2.9 \pm 0.1^{\text{ns}}$ |
|  | 250 | 3 ♀ | 5380 | 182 | $3.7 \pm 0.8^{\text{ns}}$ |
|  |  | 3 ♂ | 11 746 | 575 | $4.9 \pm 0.9^{\text{ns}}$ |
| CP | 40 | 3 ♀ | 3363 | 98 | $2.9 \pm 0.0^{\text{ns}}$ |
|  |  | 3 ♂ | 3560 | 118 | $3.3 \pm 0.4^{\text{ns}}$ |

b.w., body weight; MI, mitotic index; M ± SEM, mean ± standard error of mean; control: 0.9% NaCl; CP, cyclophosphamide (positive control); ns, non-significant.
*Significantly different from control at $p < 0.05$.
**Significantly different from control at $p < 0.001$.
***Significantly different from control at $p < 0.0001$.

Figure 2. MN test of the bone marrow cells in Swiss albino mice. The incidence of micronucleated polychromatic erythrocytes (MN-PCE) per 1000 PCEs at different concentrations of EHNs in (a) female and (b) male Swiss mice, respectively. No statistically significant difference was observed in EHNs treated group compared to control (0.9% NaCl) in female and male Swiss mice. CP: cyclophosphamide was used as a positive control experiment.
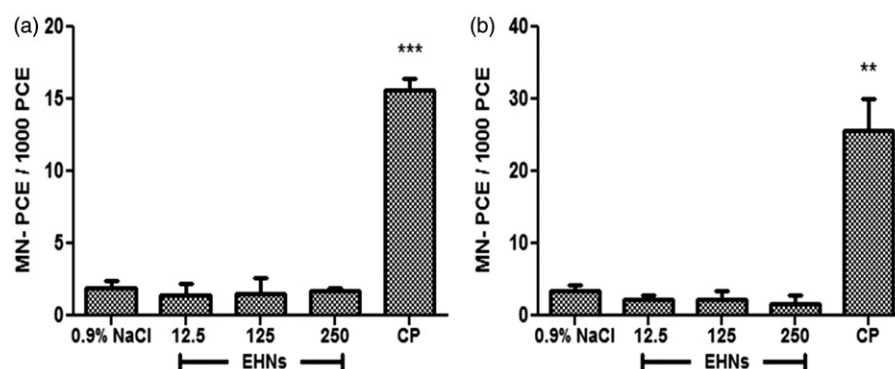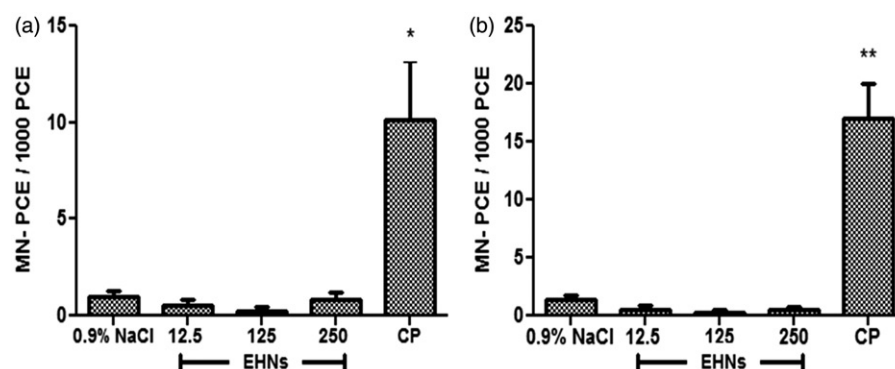


Figure 3. MN test of the peripheral blood cells in Swiss albino mice. The incidence of micronucleated polychromatic erythrocytes (MN-PCE) per 1000 PCEs at different concentrations of EHNs in (a) female and (b) male Swiss mice, respectively. No statistically significant difference was observed in EHNs treated group compared to control (0.9% NaCl) in female and male Swiss mice.



MN-PCE per 1000 PCE in response to all the dose treatments in both male and female is shown in Figure 2.

### Peripheral blood MN test

Peripheral blood MN test was conducted 30 h post-EHNs treatment to estimate the presence of MNs due to effect of the test compounds. The presence of MN induced in peripheral blood (Figure 3a and b) was found to be very less in comparison to MN induced in bone marrow cells of the negative and positive control treatment groups of Swiss mice (Figure 2a and b). Figure 3(a) and (b) and Table S2 represent the results of peripheral blood MN

assay in EHNs-treated female (Figure 3a) and male (Figure 3b) Swiss albino mice. The group that received CP exhibited significantly high percentage of MN in female ($p < 0.05$) (Figure 3a) and male ($p < 0.001$) mice (Figure 3b) when compared to the negative control group. The group that was injected with 12.5 mg/kg b.w. EHNs showed no significant difference in MN-PCE per 1000 PCE between female ($0.5 \pm 0.3^{\text{ns}}$) and male ($0.5 \pm 0.3^{\text{ns}}$) mice in comparison with the corresponding groups injected with 0.9% NaCl. Similar trend was observed with 125 mg/kg b.w. treated group that showed no major significant difference in female ($0.2 \pm 0.2^{\text{ns}}$) and male ($0.2 \pm 0.2^{\text{ns}}$) groups as compared to 0.9% NaCl treated group. Interestingly, the MN-PCE
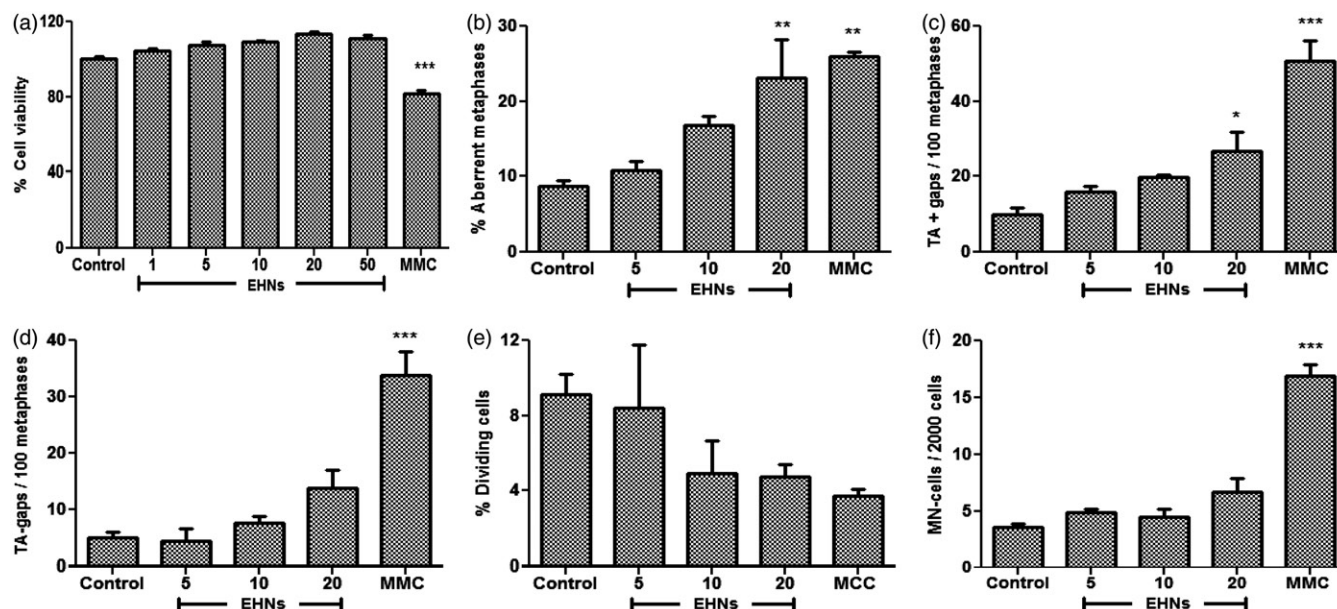
Figure 4. *In vitro* genotoxicity evaluation of EHNs in CHO cells. (a) MTT (cell viability) assay in CHO cells incubated with EHNs, (b–d) CAs observed in CHO cells post-treatment with EHNs (5, 10, 20 µg/mL) and MMC 0.8 µg/mL = 2.5 µM. (b) EHNs-20 µg/mL treated cells show significant the percentage of aberrant metaphases and (c) total aberrations including gaps/100 metaphases, whereas (d) total aberrations excluding gaps/100 metaphases was not found to be significant in CHO cells 24 h post-EHNs treatment, respectively. (e) The percentage of dividing cells was found to decrease with increasing concentration of EHNs, but the difference remains insignificant. (f) The incidence of micronucleated cells (MN-cells) per 2000 cells at different concentrations of EHNs in CHO cells was not significantly differed compared to control untreated cells for 24 h. *, **, *** indicate that there was a significant difference between the treatment and their concurrent control at $p < 0.05$, $p < 0.001$, $p < 0.0001$, correspondingly.

per 1000 PCE was also very low and non-significant in 250 mg/kg treated female ($0.8 \pm 0.4^{ns}$) and male ($0.5 \pm 0.2^{ns}$) mice group in comparison with the negative control group mice. All the three groups that received three different doses of EHNs showed very less number of MN compared to the negative control in both female (Figure 3a) and male (Figure 3b) groups, which could be attributed to the natural DNA repair mechanism attained during the migration of PCE from bone marrow to peripheral blood. The graphical representation of the tabular results of peripheral blood MN-PCE per 1000 PCE in response to all the dose treatments in both male and female is shown in Figure 3. The representative images of the normal and micronucleated PCE from bone marrow and peripheral blood cells observed in our study are shown in Figure S7.

### *In vitro* cytotoxicity and genotoxicity evaluation of EHNs in CHO cells

We performed the cytogenetic toxicity study of EHNs toward CHO cells, in order to compare with the *in vivo* results in Swiss mice. The CHO cells are selected for the genotoxicity evaluation of EHNs *in vitro* as they are considered as a normal cell and previously well reported for performing cytotoxicity and geno-toxicity studies (Hittelman & Rao, 1974; Mitchell, 1988). The systematic genotoxicity study in CHO cells consists of CAs, MI and MN test. Initially, we carried out cell viability assay towards CHO cells in order to check the cytotoxicity effect of EHNs.

#### *MTT assay*

The MTT assay was performed to investigate the viability of CHO cells in response to EHNs treatment. The results presented in Figure 4(a) clearly demonstrated an increased cell viability of CHO cells incubated with EHNs in a dose-dependent manner (1–50 µg/mL). These results also suggest the bio-compatibility and non-toxic behavior of EHNs toward CHO cells.

MMC, a cytotoxic drug that was used as a positive control experiment reduced the viability of CHO cells compared to control untreated cells.

#### In vitro *CA assay*

The effect of different concentrations of EHNs (5, 10 and 20 µg/mL) on chromosomes was evaluated using the CA assay. The results are represented in Figure 4(b)–(d) and Table S3. The results demonstrate that EHNs induced a dose-dependent increase in the number of aberrant metaphases, total number of aberration including gaps and excluding gaps. Among the three concentrations tested, EHNs at lower concentrations (5–10 µg/mL) do not show any significant increase in the toxicity while compared to control untreated cells. However, EHNs at highest concentration (20 µg/mL) showed significant increase in the total number of aberrations ($p < 0.001$) and aberration including gaps ($p < 0.05$). The positive control MMC showed high significant difference in the percentage of aberrant metaphases ($p < 0.001$) and total aberrations (including and excluding gaps) ($p < 0.0001$) in comparison to control untreated cells. Representative images of metaphase spreads of CHO cells observed in CA assay are presented in Figure S8.

#### *Mitotic index*

The MI is a measure of total number of dividing cells in a population. The CHO cells treated with EHNs showed decrease in percentage dividing cells at all the three concentrations (5, 10 and 20 µg/mL), but the difference is statistically insignificant when compared with the untreated group, as shown in Figure 4(e). The numerical data have been presented in Table S4.

#### In vitro *MN assay*

The results presented in Figure 4(f) and Table S5 demonstrated that EHNs do not induce significant MN even at highest dose
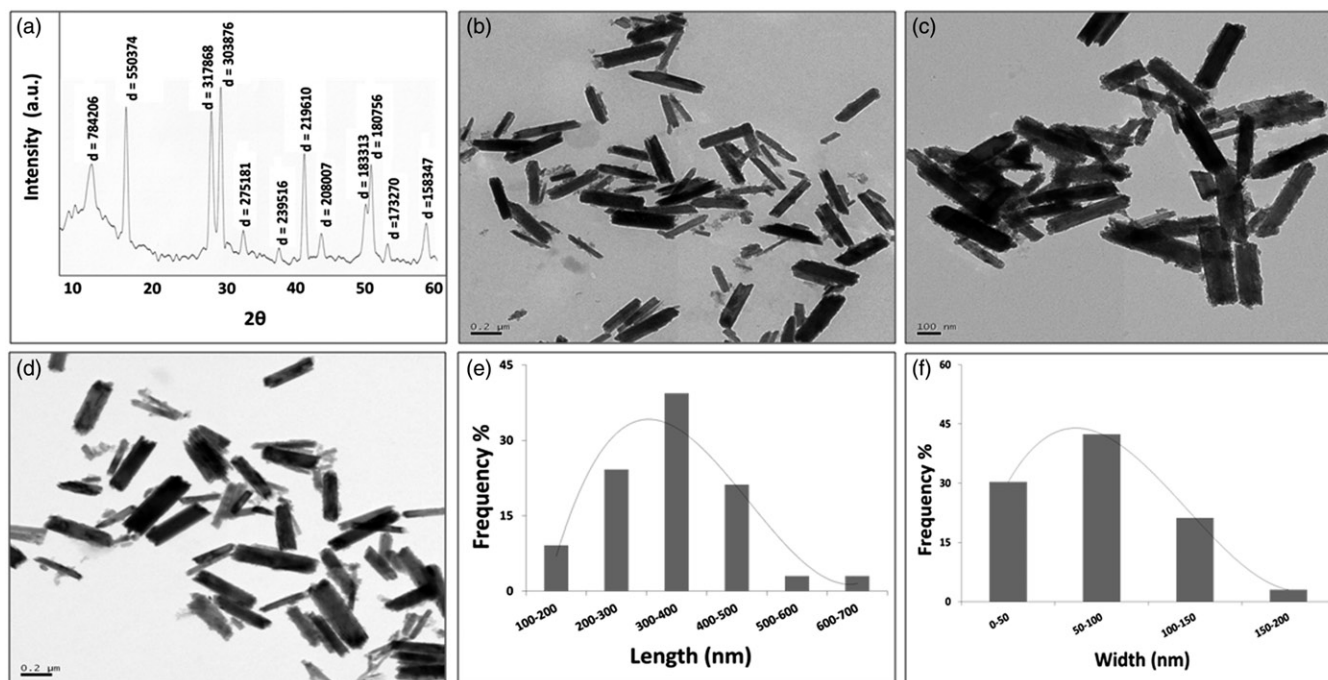
Figure 5. Secondary physico-chemical characterization of nanorods and its fate in mouse serum. (a) The XRD analysis of EHNs incubated in serum for 24 h shows their crystallinity. (b–d) The TEM images of EHNs incubated in (b) Serum-6 h, (c) Serum-24 h and (d) Serum-48 h show the clear rod shape morphology of EHNs, which is even stable up to 48 h of incubation in physiological solutions such as mouse serum. The particle size distribution (e–f) of EHNs in serum 48 h has been calculated from the TEM images using IMAGE J software, which demonstrate the average (e) length and (f) width of 300–400 and 50–100 nm, respectively.

(20 µg/mL) compared to control untreated cells. The cells treated with the positive control (MMC) showed highly significant induction of MN compared to control untreated cells. The above results suggest that EHNs is neither clastogenic nor aneugenic in nature towards CHO. Representative images of MN of CHO cells observed in MN assay are presented in Figure S9.

## Secondary physico-chemical characterization of nanorods and its fate in mouse serum

### *X-ray diffraction (XRD)*

We centrifuged (10 000 rpm for 15 min) and washed (with Millipore water) the EHNs (∼100 mg) pre-incubated in mouse serum (isolated from mouse blood) for 24 h, dried and the fine powder was submitted for XRD in order to check the existence of crystallinity after serum incubation. The XRD pattern of EHNs incubated in serum is shown in Figure 5(a), which demonstrated the pure hexagonal phase and crystalline nature of EHNs, as per reports by our group (Patra et al., 2011) and other group (Kang et al., 2014). These results suggest that EHNs maintain their crystalline nature and stable form even at physiological pH conditions.

### *TEM and DLS analyses*

We have collected the EHNs after incubation with mouse serum for different time points (6–48 h) and submitted for TEM analysis in order to check the effect of serum (physiological buffer) on morphology of the nanorods. Another set of samples was submitted for DLS analysis. The TEM images of EHNs incubated in serum for 6–48 h (Figure 5b–d) showed clear rod shape morphology of EHNs even after 48 h of serum incubation. The size distribution of EHNs in serum after 48 h incubation was done using IMAGE J software (Figure 5e–f), which demonstrated that major population of the nanorods fall in the size range of length 300–400 nm and width of 50–100 nm, which

is slightly increased compared to the size of EHNs in TE suspension.

The stability of the EHNs in physiological solutions in a time-dependent manner (6–48 h) was estimated using the DLS analysis. The average particle size of EHNs incubated in mouse serum analyzed using DLS is shown in Table S6, which showed that there was no significant difference in the average particle size of EHNs incubated in serum for 6–48 h. Altogether, the results demonstrate that these nanorods are stable at physiological pH and maintained their size and shape even after 48 h of incubation in serum, indicating their high stability.

### Bio-distribution of EHNs in Swiss mice

The analysis of bio-distribution of EHNs in the Swiss mice was performed using the ICP-OES analysis. The results (Figure 6) clearly showed the distribution of europium (µg/g) to blood and bone marrow which are the main evaluation target sites for MN and CA assay in the present study. The distribution of EHNs was also observed in various other organs such as liver, kidney, spleen and feces excreted. While comparing the bio-distribution of EHNs between 6 and 24 h post-treatment, it was observed that at 6 h study, trace amount of europium was noticed in spleen, liver and kidney, whereas below detection (BD) limit of europium was observed in blood and bone marrow. However, distribution of europium was noticed after 24 h injection in organs such as spleen, liver and kidney including blood and bone marrow, which are the target sites for the evaluation of genotoxicity assays. The presence of considerable amount of europium in feces confirmed the excretion of the material from the mouse body. So, the above results confirm that EHNs was circulated, distributed and excreted from the mouse body.

### Discussion

Recent reports by our group suggest the future application of EHNs for the development of alternative treatment strategy in

Figure 6. Determination of bio-distribution of EHNs in Swiss albino mice. The bio-distribution of europium element (µg/g) in different organs (liver, spleen and kidney), blood, bone marrow and feces of Swiss albino mice sacrificed after intraperitonial injection for 6 h ($n = 3$ male and $n = 3$ female) and 24 h ($n = 3$ male and $n = 3$ female) with EHNs (250 mg/kg b.w.), analyzed by ICP-OES.
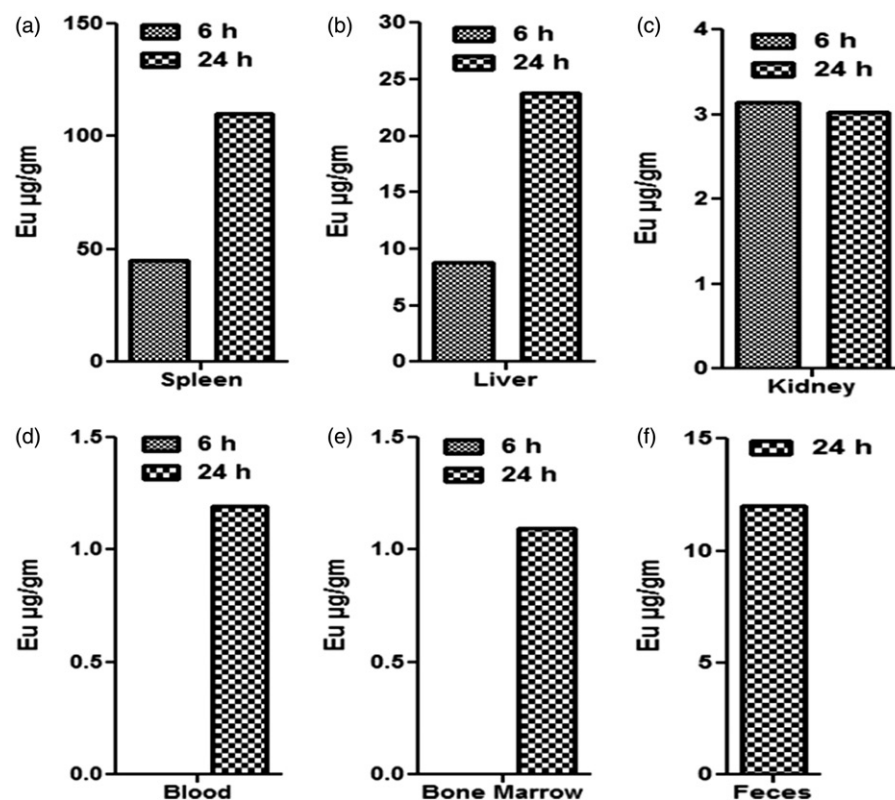


cardiovascular-related diseases, where angiogenesis plays an important role (Kim et al., 2011; Nethi et al., 2015; Patra et al., 2008a, 2009, 2011; Wei et al., 2014). Considering their enormous significance in biomedical applications, there is an emergent need to understand their *in vivo* genotoxicity to translate these nanoparticles for clinical applications. The present study aimed to evaluate various endpoints like *in vivo* cell cycle analysis (FACS), bone marrow CA test, MI and MN test both from bone marrow and peripheral blood of Swiss albino mice to provide valuable information on overall genotoxic potential of EHNs. The EHNs were synthesized based on our previous reports, along with the detailed physico-chemical characterization. XRD analysis indicated the pure crystalline nature of the compound as all the diffraction peaks indexed to a hexagonal phase (Patra et al., 2008a, 2011).TEM analysis showed the rod shape morphology of these nanoparticles with an average size of about 200–300 nm in length and 40–80 nm in diameter. The *in vivo* biochemical and histopathological studies previously reported by our group show mild to non-toxic nature of these nanorods up to a dose range of 125 g/kg b.w. in C57BL/6 mice, where the bio-distribution of EHNs in various organs of mice has also been demonstrated (Patra et al., 2009). Based on their small size, EHNs possess high tendency to accumulate in the bone marrow, in accordance with the previous reports on nanoparticles following similar size range (Moghimi, 1995), which is confirmed by the ICP-OES analysis of bone marrow in the present study.

In order to further investigate the effects of the EHNs at chromosomal level, we carried out the *in vivo* cytogenetic toxicity studies in Swiss albino mice to completely understand the safety and toxicity aspects of these nanorods. Even though the therapeutic dose of EHNs required to achieve the desired effect is much lower, for toxicity studies we need to use much higher doses to reflect their adverse accidental exposures to humans. Based on these considerations, three different doses of EHNs 12.5, 125 and 250 mg/kg b.w. were selected which reflect the dose range from a minimum therapeutic dose to a highest unintended

exposure. CP was used as a positive control (dose of 40 mg/kg b.w.) because CP is well-reported as a genotoxic agent and has been used as the positive control for comparing the maximum induction of clastogenic and anuegenic effects (Choudhury et al., 2000). CP induced significant increase in the percentage of aberrant metaphases and total number of aberrations both including and excluding gaps ($p < 0.0001$). A significant induction of MNs was recorded in both bone marrow of female ($p < 0.0001$) and male ($p < 0.001$) and peripheral blood MN of female ($p < 0.05$) and male mice ($p < 0.001$) when compared to that of the group received 0.9% NaCl, suggesting the clastogenic effect of CP which is in agreement with our earlier reports (Jackson et al., 1996; Misra & Choudhury, 2006). Similar frequency in percentage of dividing cells was recorded when the negative control group was compared with the CP group, in agreement with our earlier reports (Balasubramanyam et al., 2009).

The group of mice administered with different concentrations of EHNs showed a dose-dependent increase in the percentage of aberrant metaphases, mostly with chromatid gaps and breaks as shown in Table 1. In the cell cycle study, it was noticed that most of the cells were found in G0/G1 phase followed by G2/M and least at S phase. Most of the CAs were of chromatid gaps and breaks with the effect of EHNs suggesting that EHNs are S-phase dependent in nature. This higher number of chromatid type aberrations of EHNs at the highest dose may be due to unrepaired lesions of G1 and G2 passed the S phase and noticed in metaphase. Most of the chemical mutagens do not induce chromosomal lesions directly, whereas lesions induced by the chemicals are generally transferred to S-phase of cell cycle and in metaphase they reflect as chromatid type gaps and breaks. In our study also most of the CAs recorded were of chromatid gaps and breaks type which result due to strand break of DNA due to incomplete excision repair (Bryant, 1998). As there was a very low induction of other types of CAs, we considered chromatid gaps and chromosome gaps as aberrations in our results.

The significant higher induction of CAs at 250 mg/kg b.w. may be due to the formation of excessive reactive oxygen species (ROS) by EHNs (Patra et al., 2011). From the results of our toxicity study, it is confirmed that EHNs is neither clastogenic nor aneugenic in nature. The induction of CAs and MNs, especially at highest doses, suggests that EHNs can be mutagenic at unusual high doses, i.e. 250 mg/kg. b.w. in Swiss mice. The possible mechanism for these mutations may be due to generation of various ROS induced by the highest dose of nanorods, interacting with DNA to cause single- or double-strand breaks (Trouiller et al., 2009; Yu & Anderson, 1997). These observations are also in agreement with our earlier reports that ROS ($H_2O_2$ and $O_2^-$) are involved in redox signaling pathways during angiogenesis in the presence of EHNs in both *in vitro* and *in vivo* systems (Patra et al., 2011). Altogether, while comparing all the three doses of EHNs-treated groups, a dose-dependent increase in the number of aberrations was observed due to the induction of excess ROS reacting with DNA strands, resulting mostly with chromatid types of aberrations.

In the MI, no statically significant change in the proliferation of the number of mitotic dividing cells in the EHNs-treated groups was observed compared with the control group. However, at high concentrations of EHNs, an increase in the number of mitotic dividing cells may be attributed to the pro-angiogenic property of EHNs (Patra et al., 2011). The results of MI analysis showed the non-cytotoxic nature of EHNs towards bone marrow cells. Probably, high percentage of MI observed in bone marrow cells, especially at two higher doses, was due to the simulation of cell proliferation by EHNs. These results were also in agreement with cell cycle analysis that EHNs do not arrest cells at any of the phases of cell cycle when compared to positive and negative control groups.

MN test detects the clastogenic and aneugenic potential of the chemical. These MNs are formed due to acentric fragments, whole chromosomes or chromatids during mitotic division process. Two different sources were considered for the analysis of MN, i.e. PCEs from bone marrow and peripheral blood after 30 h post-EHNs treatment. The results shown in Tables S1 and S2 indicated that all the three concentrations of EHNs-induced MN in bone marrow cells but not statistically significant when compared with the negative control, suggesting the non-clastogenic nature of EHNs. Similarly, there is no dose–response increase in the number of MNs in EHNs-treated group in PCE from peripheral blood. It was interesting to note that, the induction of MN-PCE of peripheral blood is very less when compared to MN-PCE of bone marrow. This less number of MN in peripheral blood may be due to the repair of the affected cells in bone marrow or grossly affected cells being eliminated in the bone marrow before reaching the peripheral blood (Table S2). Also, the selective removal of micronucleated erythrocytes by the spleen (Cammerer et al., 2007) supports the observation of less MN in the peripheral blood. In the present study, mostly small sized MNs were observed which may be attributed to chromatid types of breaks, fragments or minutes (Fenech & Bonassi, 2011). There was no correlation between the number of aberrant metaphases, number of aberrations including/excluding gaps with induction of MNs in both male and female EHNs-treated groups. The overall information of MN induced by EHNs, both from bone marrow and peripheral blood, suggests that EHNs possess neither clastogenic nor aneugenic nature.

In order to extrapolate our studies to *in vitro* systems, we have performed all the standard genotoxicity assays (CA, MI and MN assay) to evaluate the cytogenetic toxicity of EHNs in CHO cells. Among all the three concentrations of EHNs tested on CHO cells, only the highest dose (20 μg/mL of EHNs) induced significant increase in the percentage of aberrant metaphases ($p < 0.001$) and also percentage of aberrations including gaps ($p < 0.05$), mostly with chromatid types (gaps and breaks) that may occur due to the effect of EHNs on the late S or G2 phase of the cell cycle. These results suggested that ENHs was not clastogenic and its toxicity was mostly S-phase dependent in nature in CHO cells (Mosesso et al., 2013). The MI of CHO cells in all the three concentrations of EHNs was lowered but was not significantly differed compared with untreated cells. The reduction of MI especially at two higher concentrations of EHNs, i.e. 10 and 20 μg/mL may be due to the delay in DNA repair mechanisms or grossly affected cells which may have been eliminated before entering to mitosis. The EHNs induced MN formation in CHO cells similar to that observed in untreated cells. It well known that the MNs induction is a consequence of major CAs or impairment of spindle fibers (Fenech et al., 2011; Shimizu, 2011). Therefore, in the present study, very less incidence of major CAs like fragments, minutes or aneuploidy was noticed, which corroborate with the low incidence of number of micronucleated cells at all the concentrations of EHNs used.

The results of all the genotoxicity evaluations (CA, MI and MN assay) of EHNs in CHO cells were in agreement with our *in vivo* cytogenetic toxicity study in Swiss albino mice. Totally, the above cytogenetic toxicity studies on CA, MI and MN confirmed that EHNs were non-clastogenic, non-mutagenic and non-aneugenic in nature and can be safely used for bio-medical application as a drug.

Finally, to understand the bio-distribution of europium in Swiss albino mice, the highest dose, i.e. 250 mg/kg b.w. was selected and assessed at two time intervals (6 and 24 h). This highest dose was selected based on our genotoxicity study of europium in Swiss mice, where maximum cytogenetic toxicity was noticed at 250 mg/kg b.w. compared to 12.5 and 125 mg/kg b.w after 24 h exposure. The ICP-OES results clearly demonstrated a low amount of europium detection in spleen and liver and BD limit of europium in blood and bone marrow after 6 h of (i.p.) injection of EHNs. At 24 h post-EHNs treatment, higher amount of europium was noticed in spleen, liver followed by considerable amount in blood and bone marrow. Interestingly, there was no significant change in the amount of europium accumulation in kidney between 6 and 24 h treatment. Moreover, the presence of europium in feces collected till 24 h clearly suggested that the europium is excreted from the mouse body. The accumulation of europium in liver and spleen may be due to the reticuloendothelial system, which might be playing a vital role in absorption of europium. These observations were in agreement with our previous reports, where higher amount of EHNs was accumulated in liver, spleen and lungs after exposure of EHNs at 125 mg/kg b.w. to C57BL/6 mice in both acute and chronic studies (Patra et al., 2009).

## Conclusion

We have synthesized the EHNs using a modified microwave method and well-characterized them by several analytical techniques. We have evaluated the *in vivo* cytogenetic toxicity of EHNs in Swiss albino mice in order to understand the mechanism of toxicity of EHNs and establish its biosafety on long-term basis for future clinical perspectives. The results of the study suggest that administration of EHNs (i.p.) at the selected dose range is safe with no evidence of gross genetic damage. The genetic damage in the form of CAs and MNs induction is mostly caused at unusual highest dose of EHNs (250 mg/kg/b.w.). Considering the role of angiogenesis and its market value on our healthcare system, we believe that EHNs could be useful in the development of new approaches for the treatment of cardiovascular-related diseases.

## Declaration of interest

## References

Adler ID. 1980. A review of the coordinated research effort on the comparison of test systems for the detection of mutagenic effects, sponsored by the E.E.C. Mutat Res 74:77–93.

Alivisatos P. 2004. The use of nanocrystals in biological detection. Nat Biotechnol 22:47–52.

Balasubramanyam A, Sailaja N, Mahboob M, Rahman MF, Misra S, Hussain SM, Grover P. 2009. Evaluation of genotoxic effects of oral exposure to aluminum oxide nanomaterials in rat bone marrow. Mutat Res 676:41–7.

Barui AK, Veeriah V, Mukherjee S, Manna J, Patel AK, Patra S, et al. 2012. Zinc oxide nanoflowers make new blood vessels. Nanoscale 4: 7861–9.

Boisselier E, Astruc D. 2009. Gold nanoparticles in nanomedicine: preparations, imaging, diagnostics, therapies and toxicity. Chem Soc Rev 38:1759–82.

Bonassi S, Znaor A, Ceppi M, Lando C, Chang WP, Holland N, et al. 2007. An increased micronucleus frequency in peripheral blood lymphocytes predicts the risk of cancer in humans. Carcinogenesis 28:625–31.

Bryant PE. 1998. Mechanisms of radiation-induced chromatid breaks. Mutat Res 404:107–11.

Cammerer Z, Elhajouji A, Kirsch-Volders M, Suter W. 2007. Comparison of the peripheral blood micronucleus test using flow cytometry in rat and mouse exposed to aneugens after single dose applications. Mutagenesis 22:129–34.

Choudhury RC, Das B, Misra S, Jagdale MB. 2000. Cytogenetic toxicity of vincristine. J Environ Pathol Toxicol Oncol 19:347–55.

Clahsen PC, van de Velde CJ, Duval C, Pallud C, Mandard AM, Delobelle-Deroide A, et al. 1999. The utility of mitotic index, oestrogen receptor and Ki-67 measurements in the creation of novel prognostic indices for node-negative breast cancer. Eur J Surg Oncol 25:356–63.

Coccini T, Manzo L, Roda E. 2013. Safety evaluation of engineered nanomaterials for health risk assessment: an experimental tiered testing approach using pristine and functionalized carbon nanotubes. ISRN Toxicol 2013:825427.

Dai H, Zhou Y, Liu Q, Li Z, Bao C, Yu T, Zhou Z. 2012. Controllable growth of dendritic ZnO nanowire arrays on a stainless steel mesh towards the fabrication of large area, flexible dye sensitized solar cells. Nanoscale 17:5454–60.

Dhawan A, Taurozzi JS, Pandey AK, Shan W, Miller SM, Hashsham SA, Tarabara VV. 2006. Stable colloidal dispersions of C60 fullerenes in water: evidence for genotoxicity. Environ Sci Technol 40:7394–401.

Di Virgilio AL, Reigosa M, Arnal PM, Fernandez Lorenzo de Mele M. 2010. Comparative study of the cytotoxic and genotoxic effects of titanium oxide and aluminium oxide nanoparticles in Chinese hamster ovary (CHO-K1) cells. J Hazard Mater 177:711–18.

Fenech M, Bonassi S. 2011. The effect of age, gender, diet and lifestyle on DNA damage measured using micronucleus frequency in human peripheral blood lymphocytes. Mutagenesis 26:43–9.

Fenech M, Kirsch-Volders M, Natarajan AT, Surralles J, Crott JW, Parry J, et al. 2011. Molecular mechanisms of micronucleus, nucleoplasmic bridge and nuclear bud formation in mammalian and human cells. Mutagenesis 26:125–32.

Franchitto, A, Pichierri P, Mosesso P, Palitti F. 1998. Caffeine effect on the mitotic delay induced by G2 treatment with UVC or mitomycin C. Mutagenesis 13:499–505.

Gao XH, Cui YY, Levenson RM, Chung LWK, Nie SM. 2004. *In vivo* cancer targeting and imaging with semiconductor quantum dots. Nat Biotechnol 22:969–76.

Giljohann DA, Seferos DS, Daniel WL, Massich MD, Patel PC, Mirkin CA. 2010. Gold nanoparticles for biology and medicine. Angew Chem Int Ed 49:3280–94.

Hittelman WN, Rao PN. 1974. Bleomycin-induced damage in prematurely condensed chromosomes and its relationship to cell cycle progression in CHO cells. Cancer Res 34:3433–9.

Ishidate Jr M, Miura KF, Sofuni T. 1998. Chromosome aberration assays in genetic toxicology testing *in vitro*. Mutat Res 404:167–72.

Jackson MA, Stack HF, Waters MD. 1996. Genetic activity profiles of anticancer drugs. Mutat Res 355:171–208.

Kang JG, Jung Y, Min BK, Sohn Y. 2014. Full characterization of Eu(OH)(3) and Eu2O3 nanorods. Appl Surf Sci 314:158–65.

Killmann SA, Cronkite EP, Fliedner TM, Bond VP, Brecher G. 1963. Mitotic indices of human bone marrow cells. II. The use of mitotic indices for estimation of time parameters of proliferation in serially connected multiplicative cellular compartments. Blood 21:141–63.

Kim JH, Patra CR, Arkalgud JR, Boghossian AA, Zhang J, Jae-Hee H, et al. 2011. Single molecule detection of H2O2 mediating angiogenic redox signaling on fluorescent single-walled carbon nanotube array. ACS Nano 5:7848–57.

Krishna G, Hayashi M. 2000. *In vivo* rodent micronucleus assay: protocol, conduct and data interpretation. Mutat Res 455:155–66.

Kumar A, Vemula PK, Ajayan PM, John G. 2008. Silver-nanoparticle-embedded antimicrobial paints based on vegetable oil. Nat Mater 7:236–41.

Lewinski N, Colvin V, Drezek R. 2008. Cytotoxicity of nanoparticles. Small 4:26–49.

Li M, Zhu Q, Hu C, Giesy JP, Kong Z, Cui Y. 2011. Protective effects of eicosapentaenoic acid on genotoxicity and oxidative stress of cyclophosphamide in mice. Environ Toxicol 26:217–23.

Liu Y, Zhang N. 2012. Gadolinium loaded nanoparticles in theranostic magnetic resonance imaging. Biomaterials 33:5363–75.

Mazumdar M, Giri S, Giri A. 2011. Role of quercetin on mitomycin C induced genotoxicity: analysis of micronucleus and chromosome aberrations *in vivo*. Mutat Res 721:147–52.

Misra S, Choudhury RC. 2006. Vitamin C modulation of cisplatin-induced cytogenotoxicity in bone marrow, spermatogonia and its transmission in the male germline of Swiss mice. J Chemother 18: 182–7.

Mitchell DL. 1988. The relative cytotoxicity of (6-4) photoproducts and cyclobutane dimers in mammalian cells. Photochem Photobiol 48: 51–7.

Moghimi SM. 1995. Exploiting bone-marrow microvascular structure for drug-delivery and future therapies. Adv Drug Deliv Rev 17: 61–73.

Mosesso P, Cinelli S, Natarajan AT, Palitti F. 2013. *In vitro* cytogenetic assays: chromosomal aberrations and micronucleus tests. Genotoxicity Assessment: Methods Mol Biol 1044:123–46.

Mulder WJM, Fayad ZA. 2008. Nanomedicine captures cardiovascular disease. Arterioscl Throm Vas 28:801–2.

Nethi SK, Mukherjee S, Veeriah V, Barui AK, Chatterjee S, Patra CR. 2014. Bioconjugated gold nanoparticles accelerate the growth of new blood vessels through redox signaling. Chem Commun 50: 14367–70.

Nethi SK, Veeriah V, Barui AK, Rajendran S, Mattapally S, Misra S, et al. 2015. Investigation of molecular mechanisms and regulatory pathways of pro-angiogenic nanorods. Nanoscale 7:9760–70.

Obregon ID, Betts-Obregon BS, Yust B, Pedraza F, Ortiz A, Sardar D, Tsin AT. 2013. Effect of silver coating on barium titanium oxide nanoparticle toxicity. Adv Mater Res 787:404–7.

Patra CR, Abdel Moneim SS, Wang EF, Dutta S, Patra S, Eshed M, et al. 2009. *In vivo* toxicity studies of europium hydroxide nanorods in mice. Toxicol Appl Pharmacol 240:88–98.

Patra CR, Bhattacharya R, Patra S, Vlahakis NE, Gabashvili A, Koltypin Y, et al. 2008a. Pro-angiogenic properties of europium(III) hydroxide nanorods. Adv Mater 20:753–6.

Patra CR, Bhattacharya R, Wang EF, Katarya A, Lau JS, Dutta S, et al. 2008b. Targeted delivery of gemcitabine to pancreatic adenocarcinoma using cetuximab as a targeting agent. Cancer Res 68:1970–8.

Patra CR, Kim JH, Pramanik K, d'Uscio LV, Patra S, Katusic ZS, et al. 2011. Reactive oxygen species driven angiogenesis by inorganic nanorods. Nano Lett 11:4932–8.

Piao MJ, Kang KA, Lee IK, Kim HS, Kim S, Choi JY, et al. 2011. Silver nanoparticles induce oxidative cell damage in human liver cells through inhibition of reduced glutathione and induction of mitochondria-involved apoptosis. Toxicol Lett 201:92–100.

Porcel E, Liehn S, Remita H, Usami N, Kobayashi K, Furusawa Y, et al. 2010. Platinum nanoparticles: a promising material for future cancer therapy? Nanotechnology 21:85103.

Rithidech KN, Golightly M, Whorton E. 2008. Analysis of cell cycle in mouse bone marrow cells following acute *in vivo* exposure to 56Fe ions. J Radiat Res 49:437–43.

Schmid W. 1975. The micronucleus test. Mutat Res 31:9–15.

Schwartz PS, Waxman DJ. 2001. Cyclophosphamide induces caspase 9-dependent apoptosis in 9L tumor cells. Mol Pharmacol 60:1268–79.

Shimizu N. 2011. Molecular mechanisms of the origin of micronuclei from extrachromosomal elements. Mutagenesis 26:119–23.

Sreedhar B, Devi DK, Neetha AS, Kumar VP, Chary KVR. 2015. Green synthesis of gum-acacia assisted gold-hydroxyapatite nanostructures – characterization and catalytic activity. Mater Chem Phys 153:23–31.

Sung HW, Sonaje K, Feng SS. 2011. Nanomedicine for diabetes treatment. Nanomedicine (UK) 6:1297–300.

Tiwari PM, Eroglu E, Bawage SS, Vig K, Miller ME, Pillai S, et al. 2014. Enhanced intracellular translocation and biodistribution of gold nanoparticles functionalized with a cell-penetrating peptide (VG-21) from vesicular stomatitis virus. Biomaterials 35:9484–94.

Trouiller B, Reliene R, Westbrook A, Solaimani P, Schiestl RH. 2009. Titanium dioxide nanoparticles induce DNA damage and genetic instability *in vivo* in mice. Cancer Res 69:8784–9.

Tsuji JS, Maynard AD, Howard PC, James JT, Lam CW, Warheit DB, Santamaria AB. 2006. Research strategies for safety evaluation of nanomaterials, part IV: risk assessment of nanoparticles. Toxicol Sci 89:42–50.

Wei PF, Zhang L, Nethi SK, Barui AK, Lin J, Zhou W, et al. 2014. Accelerating the clearance of mutant huntingtin protein aggregates through autophagy induction by europium hydroxide nanorods. Biomaterials 35:899–907.

Yan RX, Park JH, Choi Y, Heo CJ, Yang SM, Lee LP, Yang PD. 2012. Nanowire-based single-cell endoscopy. Nat Nanotechnol 7: 191–6.

Yu TW, Anderson D. 1997. Reactive oxygen species-induced DNA damage and its modification: a chemical investigation. Mutat Res 379: 201–10.

**Supplementary material available online**
Supplementary Figures S1–S7 and Tables S1–S6.